The Visual Computer

Virtual spectrophotometric measurements for biologically and physically based rendering

Gladimir V.G. Baranoski[1],
Jon G. Rokne[2],
Guangwu Xu[3]

[1] Department of Computer Science, University of Waterloo, Canada
[2] Department of Computer Science, The University of Calgary, Canada
[3] Diversinet Corporation, Toronto, Canada

Published online: 18 September 2001

Virtual spectrophotometric measurements have important applications in biologically and physically based rendering. These measurements are used to evaluate reflectance and transmittance models through comparisons with actual spectrophotometric measurements. Moreover, they are also used to generate spectrophotometric data, which are dependent either on the wavelength or on the illuminating geometry of the incident radiation, from previously validated models. In this paper the ray casting based formulation for virtual spectrophotometers is discussed, and an original ray density analysis is presented, which increases the efficiency of these virtual devices. Specifically, a mathematical bound based on probability theory is proposed to determine the number of rays needed to obtain asymptotically convergent readings in the shortest possible computation time. Practical experiments are provided which illustrate the validity and usefulness of the proposed approach.

Key words: Spectral measurements – Ray density – Rendering

1 Introduction

The group of measurements necessary to characterize both the color and surface finish of an object is called the *measurement of appearance* of that object [20]. This group of measurements involves the spectral energy distribution of propagated light, measured in terms of reflectance and transmittance, and the spatial distribution of that light, measured in terms of the bidirectional reflectance distribution function (BRDF) and the bidirectional transmittance distribution function (BTDF). As stated by [20], the variations in the spectral energy distribution affect appearance characteristics such as hue, lightness and saturation, while the changes in the spatial distribution affect appearance characteristics such as gloss, reflection haze, transmission haze, luster and translucency. The measurement of these appearance characteristics is crucial for realistic rendering applications, as was noted in the recent Workshop on Rendering, Perception and Measurement [11].

There are many scattering models in the computer graphics literature classified as reflectance and transmittance models. This classification is in many cases not entirely accurate since they only model the BRDF and BTDF using reflectance and transmittance values, which correspond to input data, as scaling factors or "weights" for the spatial distribution of the scattered light. For example, the multiple-layer model proposed by [17] can be used to render a maple leaf under different lighting conditions, provided its reflectances and transmittances for different wavelengths and illuminating geometries are available as data for the model. Similarly, in [4] a non-deterministic reconstruction approach is applied to a biological system (a leaf model) where the reconstruction is made on the basis of already known data. The question is now: Where do the data for the these models come from? This question highlights two important issues related to biologically and physically based rendering. First, it shows the need to develop models to compute reflectances and transmittances, especially for organic materials, as considered in [3], for example. Second, it shows the need to develop accurate and efficient spectral measurement procedures, as pointed out in the recent Workshop on Metrology and Modeling of Color and Appearance[1]. The latter issue is addressed in this paper.

A spectrophotometer is defined to be any instrument for measuring spectral distribution of reflected and transmitted radiant power, and spectrophotom-

[1] www.ciks.nist.gov/appmain.htm

Digital Object Identifier (DOI) 10.1007/s003710100127

etry is defined as the quantitative measurement of reflection and transmission properties as a function of wavelength [2]. Spectrophotometers can also be used to determine the absorption characteristics of an object as a function of wavelength. In this paper we are mostly interested in computer simulations of these devices, henceforth called virtual spectrophotometers, aimed at biologically and physically based rendering applications. However, the techniques presented in this paper can also be applied to other fields such as colorimetry, solar engineering and remote sensing.

Virtual spectrophotometers are normally implemented using ray casting algorithms combined with stochastic techniques applied to particle transport simulations [9]. The purpose of these devices is to determine the numerical value of an estimand, or expected value, to which the readings of reflectance, or transmittance, of a model converge. This estimand will correspond to a reflectance, or transmittance, value for a given wavelength and illuminating geometry. Note that we will focus on reflectance, including transmittance by analogy when discussing virtual spectrophotometric measurements since it is handled similarly to reflectance.

Virtual spectrophotometers may sometimes provide estimates with low variance with respect to the estimand in the early stages of the simulation due to their nondeterministic nature, i.e., after using a small number of sample rays. Since the value of the estimand is unknown before the simulation, these earlier estimates are not reliable, and estimates within the region of asymptotic convergence of the estimand are, therefore, desired. In fact, if one knew a priori the value of the estimand there would be no point in carrying out virtual spectrophotometric measurements. To ensure that the estimates for a given model are within the asymptotic convergence region, a brute-force approach, which consists of using a very large number of sample rays – in some cases up to 10^8 rays [12] – is usually applied. However, the application of this strategy results in a high computational overhead in terms of processing time. This overhead becomes rather prohibitive when the simulations involve a large number of measurements for different wavelengths and finer incidence sampling resolutions.

In this paper we discuss the main aspects of virtual spectrophotometry and perform a ray density analysis to determine the least number of sample rays required to obtain estimates within the region of asymptotic convergence of the estimand with high confidence, thus reducing the processing time substantially. As noted earlier, the determination of an appropriate ray density, or sample size, shall not depend on the knowledge about the value of the estimand or on its variance. This can be achieved by using the exponential Chebyshev inequality [27], adapting it to the requirements of spectrophotometric measurements aimed at rendering applications. Numerical experiments involving reflectance models with different levels of complexity illustrate its applicability. An extended abstract of the paper was presented at a conference as a poster [7].

The remainder of this paper is organized as follows. The next section provides the physics background for the discussion that follows. Section 3 outlines the practical applications of virtual spectrophotometers and describes their stochastic formulation. Section 4 discusses the applicability of inequalities usually used in particle transport simulations and introduces the exponential Chebyshev inequality to the rendering literature. Section 5 describes the procedures used in the evaluation of the usefulness of the proposed approach and discusses the results of the experiments. The paper closes with a summary and directions for future research.

2 Spectrophotometric background

2.1 Reflectance and transmittance terms

Reflectance and transmittance are important terms used in the description of the appearance of objects or surfaces. The reflectance of a given surface can be defined as the fraction of light at wavelength λ incident from a direction ψ_i that is neither absorbed into nor transmitted through the surface [26], and it is denoted by $\rho(\lambda, \psi_i)$. Similarly, the fraction of light transmitted through the surface is called the transmittance, $\tau(\lambda, \psi_i)$. The light that is neither reflected nor transmitted by the surface is absorbed. The parameter that describes the amount of absorbed light is absorptance [1], denoted by $\alpha(\lambda, \psi_i)$. The sum of the reflectance, transmittance and absorptance is one.

In computer graphics we are interested in the amount of light hitting a surface or film plane during a set period of time. Radiant power or flux, denoted by Φ (measured in watts, or joules per second), is therefore often used, as pointed out by [26]. In this context reflectance can be defined as the ratio of reflected

flux to incident flux [24]. Similarly, transmittance can be defined as the ratio of transmitted flux to incident flux.

Other important terms used in the description of appearance of objects are the reflectance and transmittance factors. The reflectance factor, denoted by R, is defined as the ratio of flux reflected from the specimen to flux reflected from a perfect reflecting diffuser under the same spectral and geometrical conditions of measurement [2]. Similarly, the transmittance factor, denoted by T, is defined as the ratio of flux transmitted by the specimen to flux transmitted by a perfect transmitting diffuser under the same spectral and geometrical conditions of measurement. There are different types of reflectance (or transmittance) depending on the incident and reflected (transmitted) solid angles associated with the incident and reflected (transmitted) beam geometry. [24] distinguish three types of solid angles: directional, conical and hemispherical. There are, therefore, nine possible combinations of solid angles resulting in nine types of reflectance. For instance, if the incident beam is collimated and the collection of the reflected flux is performed taking into account the whole hemisphere above the plane of the specimen, then directional-hemispherical reflectance is being measured.

2.2 General characteristics of actual spectrophotometers

Actual measurements of reflectance and transmittance are performed using spectrophotometers equipped with an integrating sphere [21]. An integrating sphere is usually used to measure the hemispherical reflectance factor, i.e., a reflectance factor for a hemispherical reflected solid angle [24]. The numerical values of the reflectance and the reflectance factor are, however, identical under the conditions of hemispherical collection [13].

For absolute measurements, the sphere wall is the standard, and the integrating sphere theory [14] compensates for the absolute reflectance of the sphere wall by mathematically treating the wall reflectance as unity. Hence, the hemispherical measurements made with such integrating spheres correspond to absolute values of reflectance (or transmittance), which are subject to small errors associated with factors such as aperture losses, small values of nonuniformity of sphere wall reflectance and stray reflectance from specimen mounts [29].

The precision of a real spectrophotometer is estimated by its ability to replicate a measurement for a given specimen under the same spectral and geometrical conditions [21]. The best-designed, best-constructed and best-calibrated spectrophotometers still yield results that differ from one measurement to the next. According to [23], the differences among readings should be quite small and randomly different. These differences, or uncertainties, are net results of combinations of many small fluctuations due to independent variations of different components of the instrument, different factors in the environment and how the specimen is handled. In theory, a spectrophotometer is considered to be of high precision if the spectral measurements have an uncertainty, μ, of approximately ± 0.001 [21, 23]. In practice, however, spectrophotometers usually have an absolute precision between 0.993 and 0.995 [29]. The accuracy of a spectrophotometer is measured by the ability of the device to provide, for given illuminating and viewing geometries, the true spectral reflectance and transmittance of a given specimen, apart from random uncertainties occurring in repeated measurements [21].

3 Virtual spectrophotometry

3.1 Applications

The use of virtual measurement devices gives us control over the spectral data generation from computer models and allows us to perform experiments at different sampling resolutions, which are essential requirements for rendering applications, as pointed out by [22]. In the computer graphics literature there are a reasonable number of studies of actual and virtual goniophotometers which measure BRDF and BTDF. To the best of our knowledge, there are no detailed descriptions and analyses of the performance and accuracy of virtual spectrophotometers. Moreover, when virtual measurement devices are discussed, they are usually presented in connection with a scattering model. For example, [15] have used a device for spectral and spatial measurements, a virtual goniospectrophotometer, presented as an optics model and a capture dome used in conjunction with a geometric model of surface microstructure. In this paper the formulation, accuracy and efficiency of virtual spectrophotometers are discussed independently of the reflectance and transmittance model being used.

Two applications of virtual spectrophotometers are especially relevant for biologically and physically based rendering. The first application corresponds to virtual spectrophotometric measurements aimed at the testing and evaluation of reflectance models through comparisons with actual spectrophotometric measurements. Obviously, reflectance models can be verified against measurements of real materials. However, in order to obtain the readings from the reflectance models in the first place one must perform a computer simulation of the inputs and outputs of the model, i.e., use a virtual spectrophotometer. Moreover, the formulation of this virtual device has to reproduce actual measurement conditions as faithfully as possible to minimize the introduction of bias in the comparisons. It may be argued that wildly different reflectance models can provide the same reflectance for a given illuminating, or incidence, geometry. However, for practical purposes the evaluation of a computer model will take into account how close, quantitatively and qualitatively, the overall spectral curves provided by this model are to the actual spectral curves for different measurement instances. For example, suppose that the spectral curves provided by model A have an average discrepancy of 5% with respect to the actual curves and the curves provided by model B have an average discrepancy of 30%. If the rendering pipeline has other sources of errors of small magnitude then model A is appropriate, and if the errors in the pipeline are larger then model B is a better choice assuming that this results in an overall speed improvement.

The second application corresponds to spectrophotometric data generation from previously validated models. This may involve a large number of measurements of different wavelengths and illuminating geometries. Such data can sometimes be found in the literature where actual measurements from real materials are reported. However, more often it is not available and even when it is available it is only for a restricted number of measurement configurations. For example, the most comprehensive set of experiments involving leaf optical properties performed to date [19] was limited to a small number of illuminating geometries.

Although these applications usually involve reflectance and transmittance measurements, they can be extended to other phenomena as well. For example, commercial surfaces such as paint, plastics, papers and textiles, both matte and glossy, show some degree of retroreflection, i.e., reflectance in the incident direction. This phenomenon can be measured easily using a virtual spectrophotometer when an appropriate reflectance model for such a surface is provided.

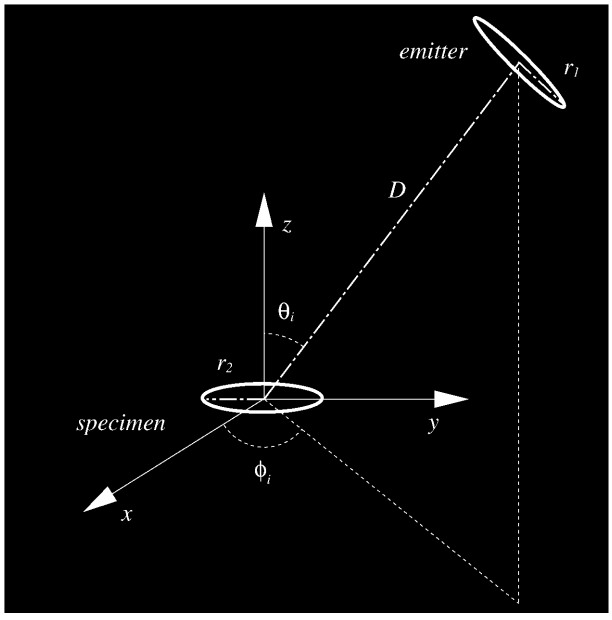

Fig. 1. Sketch of a virtual spectrophotometer

3.2 Formulation of virtual spectrophotometers

Emitters and specimens used in actual measurements usually have circular areas [12, 14, 19, 29], which can be represented by disks with radii r_1 and r_2 separated by a distance D (Fig. 1). A spectrophotometer with integrating sphere is simulated by sending (or shooting) sample rays from the emitter towards the specimen. These rays arrive at the specimen through a solid angle, $\boldsymbol{\omega}_i$, in the direction of incidence ψ_i, which is given by a pair of spherical coordinates (ϕ_i, θ_i) (Fig. 1). We denote the total number of sample rays used in a virtual spectrophotometric measurement by N. For the sake of compactness we may also represent the sample ray density by $\log_{10} N$.

Consider N rays shot towards the specimen for a given wavelength λ. One can assume that each ray carries the same amount of radiant power, Φ. If the total radiant power to be shot is Φ_i, then the radiant power carried by each ray is given by [26]:

$$\Phi_{\text{ray}}(\lambda) = \frac{\Phi_i(\lambda)}{N}. \quad (1)$$

Recall that reflectance describes the ratio of reflected power to incident radiant power and transmittance describes the ratio of transmitted radiant power to incident power [24]. Considering this ratio, if m rays are reflected towards the upper hemisphere Ω_r, the reflectance of the specimen with respect to a given wavelength λ of the incident light will be given by:

$$\rho(\lambda, \boldsymbol{\omega}_i, \Omega_r) = \frac{m}{N}. \quad (2)$$

Therefore, one can simply count the number of rays reflected to the upper hemisphere to determine a specimen's reflectance, i.e., a virtual spectrophotometer does not use an integrating sphere to collect the reflected rays. The specimen's transmittance is calculated in a similar manner, i.e., by counting the number of rays transmitted to the lower hemisphere.

Model-dependent issues, such as the use of weights associated with rays, will not be dealt with in this paper. In the same way that an actual spectrophotometer is completely independent of how the specimen interacts with light, a virtual spectrophotometer shall also be independent of the reflectance model being tested. Moreover, these weights are usually based on reflectances and transmittance values. As mentioned before, if we knew these values a priori there would be no point in carrying out spectrophotometric measurements.

For applications involving data generation from a previously validated model, the sample rays are collimated since we are basically measuring directional-hemispherical reflectance [24]. In this case, the sample rays have the same origin and hit the specimen at the same point. For applications involving comparisons with actual measurements, as mentioned earlier, the actual measurement conditions must be reproduced as faithfully as possible. In these situations we are measuring conical-hemispherical reflectance [24], which requires the generation of sample rays distributed angularly according to the geometrical arrangement of the surfaces used to represent the emitter and the specimen. As mentioned by [12], the incident radiation from an emitter shows no preference for one angular region over the other. So, in order to simulate these measurement conditions, the origins and targets of the rays are random points (or sample points) chosen on the disks used to represent the emitter and the specimen, respectively.

Several sampling strategies may be used to select the sample points on the disks [26]. In this paper we do not intend to determine the most accurate or the most efficient sampling strategy. The merits and drawbacks of different sampling strategies have been adequately covered elsewhere [13, 26]. We did, however, apply two different and well-known strategies to select the random points used in the first set of experiments (Sect. 5) in order to increase the scope of observations. For the same reason, we used two different reflectance models in these experiments.

One of the sampling strategies used in our experiments is based on standard *random sampling* [26]. It consists of generating sample points inside a square with sides $2r$ and throwing away points lying outside an inscribed disk of radius r [12]. The sample points in the square are generated using uniformly distributed random numbers ξ_1 and ξ_2 on the interval [0, 1] and the transformation

$$(x, y) = r(2\xi_1 - 1, 2\xi_2 - 1), \quad (3)$$

where the pair (x, y) corresponds to the coordinates of a sample point.

The other strategy used in our experiments is based on the classical Monte Carlo *stratified sampling* or *jittered sampling* [26]. It uses a warping transformation to guarantee that the sample points are reasonably equidistributed on a disk, and enables the computation of the pair (x, y) through the warping function

$$(x, y) = (2\pi\xi_1, r\sqrt{\xi_2}). \quad (4)$$

After generating the x and y coordinates of a sample point, using either approach mentioned above, the z coordinate is added. For a sample point on the specimen, z is equal to zero, and, for a sample point on the emitter, z will correspond to the distance D between the disks (Fig. 1), which is given by the distance between the emitter and the specimen mount of the integrating sphere of a real spectrophotometer. Finally, to obtain the origin of a sample ray, the corresponding sample point (x, y, z) on the emitter shall be rotated according to a specified incidence geometry given by ϕ_i and θ_i (Fig. 1).

4 Ray density analysis

The main question to be addressed when performing a virtual spectrophotometric measurement is how many rays should be cast by the emitter element, i.e., how large should N be. Using a sufficiently

large number of sample rays, one will have a high probability of obtaining estimates within the region of asymptotic convergence of the expected value of reflectance, or transmittance, being measured according to the Bernoulli theorem (Sect. 4.1). However, as shown by numerical experiments presented in Sect. 5 (Fig. 3), the processing time grows linearly with respect to the total number of sample rays N since the cost of the algorithm is constant per ray.

The purpose of the following analysis is to determine a satisfactory bound for N such that we can obtain estimates of reflectance ρ, or transmittance τ, with a higher reliability/cost ratio. In other words, we want to obtain estimates within the region of asymptotic convergence and reduce the processing time. In this context the term "satisfactory" means taking into account the uncertainty of the real spectrophotometer, whose readings we are comparing the virtual spectrophotometric measurements with, and aiming at an error tolerance for ρ, or τ, compatible with rendering requirements. Before coming to the specifics of the criterion proposed in this paper to select a satisfactory bound for N, we review some relevant concepts in the next section.

The application of Monte Carlo sampling strategies has been extensively explored in the rendering literature. As mentioned earlier, the application of accuracy evaluation techniques to Monte Carlo simulations usually presents the paradox of requiring as input value the estimand whose calculation is the goal of the simulation. Moreover, the variance of the stochastic process used to compute the estimand is not known a priori either. These drawbacks are usually overcome by pre-estimating the variance of the stochastic process, so that the accuracy evaluation techniques can be applied. In order to obtain these pre-estimated values one usually needs to cast a first set of rays in the simulation, which in turn demands some computational effort to guarantee reasonably accurate pre-estimates.

At this point we wish to remind the reader that the strategy used in this paper to determine a satisfactory bound for N assumes neither a previous knowledge of the variance nor the computation of variance pre-estimates. For this reason, we do not make specific references to previous work on the application of Monte Carlo methods and variance pre-estimation techniques presented in the rendering literature. The reader interested in a comprehensive survey on this topic is referred to [13].

4.1 Bernoulli's theorem and Chebyshev's inequality

A random variable ζ that takes two values 1 and 0 with probabilities p ("success") and q ("failure"), where $p+q=1$, is called a Bernoulli random variable [27]. A probabilistic model of k independent sampling experiments with two possible outcomes occurring with probabilities p and q is called a Bernoulli trial [28].

Suppose that $\zeta_1, \zeta_2, \ldots, \zeta_k$ are the outcomes of independent Bernoulli trials. The expectation of a Bernoulli variable ζ_i is given by

$$E(\zeta_i) = p. \tag{5}$$

As stated by [27], if we define the sum of k Bernoulli random variables as

$$S_k = \sum_{i=1}^{k} \zeta_i, \tag{6}$$

it follows that

$$E(S_k) = kp. \tag{7}$$

The relative frequency S_k/k becomes and remains close to p with probability one for sufficiently large k as stated by [10]. Jakob Bernoulli, in his posthumous book *Ars Conjectandi* (1713), published a theorem [28] that formally describes this fact. Let ϵ be the error tolerance and δ the confidence indicator. The Bernoulli theorem states that, for every $\epsilon > 0$ and $\delta > 0$, there is a number K such that, for $k = K+1, K+2, \ldots,$

$$P\left\{\left|\frac{S_k}{k} - p\right| \geq \epsilon\right\} > 1-\delta, \tag{8}$$

where $P\{w\}$ means the probability of w.

The particle transport simulation can be seen as a Bernoulli trial [8, 9]. In this context, a general result of probability theory, known as Chebyshev's inequality [10, 28], can be used to determine the number of samples needed to obtain estimates with a certain error tolerance in a strip of width ϵ. This inequality states that:

$$P\{\zeta \geq \epsilon\} \leq \frac{E(\zeta)}{\epsilon}, \qquad \forall \epsilon > 0. \tag{9}$$

From Chebyshev's inequality it can be shown [27] that

$$P\left\{\left|\frac{S_k}{k} - p\right| \geq \epsilon\right\} \leq \frac{pq}{k\epsilon^2} \leq \frac{1}{4k\epsilon^2}. \tag{10}$$

Recall from probability theory that

$$P\{|w| < \epsilon\} = 1 - P\{|w| \geq \epsilon\}. \tag{11}$$

Hence, we can rewrite the inequality given by (10) as

$$P\left\{\left|\frac{S_k}{k} - p\right| < \epsilon\right\} \geq 1 - \frac{1}{4k\epsilon^2}. \tag{12}$$

The confidence in an estimation is a given parameter (usually small). It measures the probability of achieving a tolerable error. Theoretically δ is a positive number such that

$$\delta \geq 1 - P\left\{\left|\frac{S_k}{k} - p\right| < \epsilon\right\}. \tag{13}$$

Then, to satisfy the above inequality, it is required that

$$\delta \geq \frac{1}{4k\epsilon^2}. \tag{14}$$

Therefore, from Chebyshev's inequality, the least number of sampling experiments required to obtain estimates with a confidence δ is given by

$$k_c = \left\lceil \frac{1}{4\epsilon^2\delta} \right\rceil. \tag{15}$$

4.2 Applying the exponential Chebyshev inequality to virtual spectrophotometry

The exponential Chebyshev inequality [27] can be used to obtain a more precise bound for the number of sampling experiments than the bound derived from the ordinary Chebyshev inequality described in the previous section. Assuming $w \geq 0$ and $\nu > 0$, the "exponential form" of the Chebyshev inequality states that

$$P\{w \geq \epsilon\} = P\{e^{\nu w} \geq e^{\nu\epsilon}\} \leq E\{e^{\nu(w-\epsilon)}\}. \tag{16}$$

From the exponential Chebyshev inequality it can be shown [27] that

$$P\left\{\left|\frac{S_k}{k} - p\right| \geq \epsilon\right\} \leq 2e^{-2k\epsilon^2}. \tag{17}$$

Using (11) it follows that

$$P\left\{\left|\frac{S_k}{k} - p\right| < \epsilon\right\} \geq 1 - 2e^{-2k\epsilon^2}. \tag{18}$$

From reasoning similar to that used to obtain the inequality given by (14), it follows that

$$\delta \geq 2e^{-2k\epsilon^2}. \tag{19}$$

Hence, from the exponential Chebyshev inequality, the least number of sampling experiments need to obtain estimates with a confidence δ is given by

$$k_e = \left\lceil \frac{\ln(2/\delta)}{2\epsilon^2} \right\rceil. \tag{20}$$

As mentioned by [27], using the theory of limits, it is possible to compare the bound k_c provided by the ordinary Chebyshev inequality with the bound k_e provided by the exponential Chebyshev inequality:

$$\lim_{\delta\to 0} \frac{k_c(\delta)}{k_e(\delta)} = \lim_{\delta\to 0} \frac{1}{2\delta\ln(2/\delta)} = \infty. \tag{21}$$

It is clear from the previous expression that when $\delta \to 0$, k_e is tighter than k_c. In virtual spectrophotometric measurements oftentimes one needs relatively low accuracy estimates, however. For example, illuminating engineers need solutions accurate to only 1–10%, as mentioned by [25], since humans do not perceive finer variations of light.

This accuracy requirement is also valid for spectrophotometry aimed at rendering applications. Before analyzing this issue further, we describe how the probability concepts presented so far fit into virtual spectrophotometry.

We can think of a virtual spectrophotometric reflectance measurement as a Bernoulli trial, and the sample rays as Bernoulli random variables. Viewed in this context, the reflectance ρ, or the probability of a sample ray being reflected to the upper hemisphere, corresponds to p. Also, the total number of sample rays N corresponds to k, and the number of rays m reflected to the upper hemisphere corresponds to S_k. Moreover, the uncertainty μ of the real spectrophotometer, whose readings we intend to compare the virtual spectrophotometric measurements with, can be associated with ϵ. Therefore, (12) and (18), and the bounds derived from them, can be rewritten using terms applied to virtual spectrophotometry.

For instance, (18) can be rewritten as

$$P\left\{\left|\frac{m}{N} - \rho\right| < \mu\right\} \geq 1 - 2e^{-2N\mu^2}, \tag{22}$$

and the bound on the number of sample rays derived from the exponential Chebyshev inequality can be rewritten as

$$N = \left\lceil \frac{\ln(2/\delta)}{2\mu^2} \right\rceil. \tag{23}$$

The figures presented in Table 1 show that, even for relatively low accuracy measurements, the bound

Table 1. Comparison of bounds on the number of sample rays required to obtain estimates with a confidence given by δ and $\mu = 0.005$

δ	ordinary Chebyshev $\log N$	exponential Chebyshev $\log N$
0.001	7.0	5.18
0.01	6.0	5.02
0.1	5.0	4.77

derived from the exponential Chebyshev inequality results in a number of sample rays considerably smaller than the number given by the bound derived from the ordinary Chebyshev inequality. Notice that these figures are given in a logarithmic scale. In Sect. 5 we present experiments that illustrate the applicability of the exponential Chebyshev bound in virtual spectrophotometry, and highlight the significant time savings that can be obtained from its application.

5 Results and discussion

5.1 Experimental procedures

We used reflectance models with different levels of complexity to illustrate the applicability of the proposed bound (23) for the ray density under different measurement conditions. The first model used in our experiments corresponds to a simplified reflectance model for dielectrics, similar to the one described by [26]. It essentially consists of computing the Fresnel coefficient F, using Fresnel equations [18], when a ray hits the specimen. This coefficient is compared with a random number ξ uniformly distributed on the interval $[0, 1]$. If $F \leq \xi$, then the sample ray is reflected to the upper hemisphere. This model does not account for wavelength dependency and uses the index of refraction, η, of the dielectric as parameter. For the experiments with this model we used the refractive index $\eta = 2.419$ of diamond [26].

We acknowledge the fact that this model increases the variance of the estimand by converting a known value to a probability. However, we again remind the reader that the accuracy of any specific model is not being evaluated here. Instead, we are interested in the evaluation of the reliability of the measurement procedures which are not based on the previous knowledge of the variance.

The second wavelength-dependent reflectance model is controlled by a larger number of parameters. It corresponds to an algorithmic model of light propagation in foliar tissues, the ABM [3]. Its formulation as well as the values assigned to its parameters, which in our experiments correspond to a soybean leaf, are described in [3]. Images of soybean leaves generated using foliar spectral data provided by this model in three wavelengths ($\lambda = 608$ nm, $\lambda = 551$ nm and $\lambda = 465$ nm) are shown in Fig. 6 of [5]. The wavelength chosen for the experiments in this paper was $\lambda = 551$ nm (the peak of human light sensitivity and the peak of light absorption by chlorophyll, the main foliar pigment, in the visible range).

The experiments performed to illustrate the applicability of the proposed bound for the number of sample rays were divided into two sets. In the first set we tested its application in virtual spectrophotometry aimed at the evaluation of reflectance models. As mentioned earlier, this type of application involves the comparison of virtual spectrophotometric measurements with measurements obtained using a real device. This implies that one should assign values for the dimensions of the virtual device as close as possible to the values of the actual device. The values used in our experiments ($r_1 = 8$ mm, $r_2 = 12.5$ mm and $D = 100$ mm) correspond to values available in the spectrophotometry literature [12, 23, 29].

In the second set of experiments we illustrate the suitability of the proposed bound for applications involving data generation from previously validated reflectance models. For these experiments we simulate collimated rays, i.e., all sample rays used in a given measurement for specified geometrical and spectral conditions have the same origin and hit the specimen at the same point. This type of application usually involves a large number of measurement instances, e.g., readings for polar angles of incidence, θ_i, varying from 0° to 90° in intervals of 1°. In order to observe the average magnitude of the fluctuations of the resulting curves we use the formula

$$\Delta = \frac{\sum_{i=1}^{n} |\rho_i^{(N_j)} - \rho_i^{(N_{j-1})}|}{n}, \tag{24}$$

where $\rho_i^{(N_j)}$ and $\rho_i^{(N_{j-1})}$ correspond to the current and previous reflectance estimates obtained using the respective ray densities, and n corresponds to the total number of directional-hemispherical reflectance measurement instances.

The ray casting algorithm used by the virtual spectrophotometer described in this paper has a constant

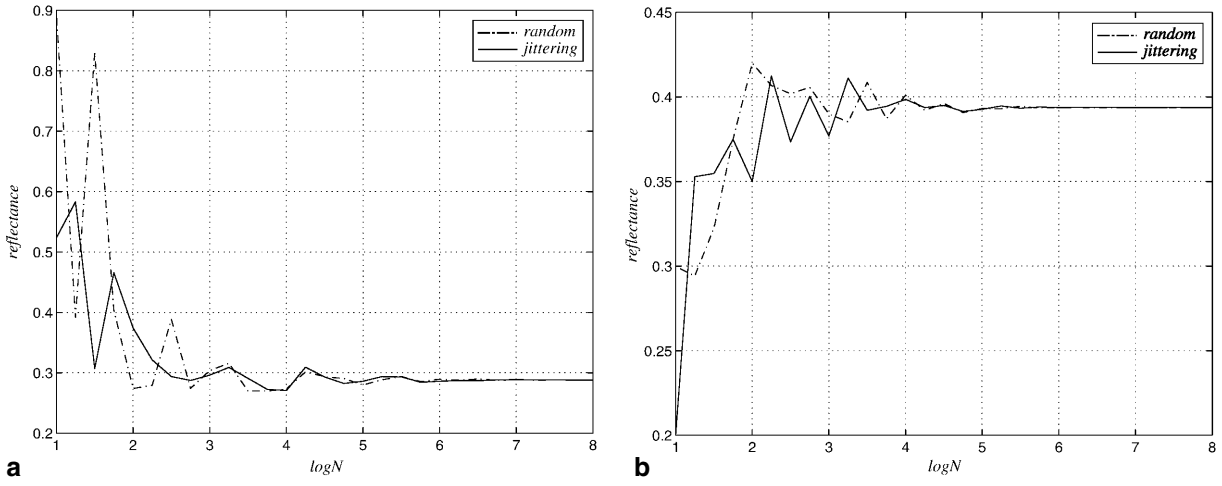

Fig. 2a,b. Reflectance estimates provided by: **a** the simplified reflectance model for dielectrics ($\eta_{\text{diamond}} = 2.419$); **b** the algorithmic reflectance model for plant leaves ($\lambda = 551$ nm)

cost per ray, i.e., there is a linear relationship between N and the cost. Notice that the graphs presented in this section are not used to show this relationship. Instead, they are presented to show that by using the number of rays given by the proposed bound (23) one can obtain asymptotically convergent estimates. Furthermore, as mentioned earlier, we represent the sample ray density by $\log_{10} N$ just for the sake of compactness.

As mentioned above – see also [25] – an accuracy of 1% is satisfactory, i.e., $\delta = 0.01$ for spectrophotometric measurements aimed at rendering applications. Also, according to data provided in the spectrophotometry literature [21, 23, 29], the absolute precision of actual spectrophotometers is around 0.995, which allows us to set $\mu = 0.005$. Applying the proposed bound, the number of sample rays required under these conditions is $N = 10^{5.02}$ (or $\log N = 5.02$).

5.2 Measurements of conical-hemispherical reflectance

Figures 2–4 present conical-hemispherical reflectance measurements for an incident direction given by $\phi_i = 0°$ and $\theta_i = 70°$, and using different ray densities. In order to increase our scope of evaluations, we applied two different sampling strategies, random and jittering-based, to select the sample points on the disks of the virtual device.

We can obtain estimates within the region of asymptotic convergence using the number of rays provided by the proposed bound, i.e., $N = 10^{5.02}$ (or $\log N = 5.02$) as we can observe in the graphs presented in Fig. 2. On the other hand, we could obtain estimates within the region of constant convergence through the application of a brute-force approach, e.g., using $N = 10^8$ (or $\log N = 8$). The graphs presented in Fig. 3 show, however, that in this case we would have a very significant increase in the processing time required for the virtual spectrophotometric measurements. This suggests that we can obtain estimates with a higher reliability/cost ratio using a ray density provided by a bound based on probability theory (Sect. 4).

Moreover, by examining the figures presented in Table 1 for $\delta = 0.01$ and the graphs presented in Fig. 4, we can also verify that the proposed bound, derived from the exponential Chebyshev inequality, allows us to obtain estimates with a higher reliability/cost ratio than the bound derived from the ordinary Chebyshev inequaglity. The practical benefit of using a tighter bound becomes even more noticeable when one works with applications involving a large number of virtual spectrophotometric measurements. In this case, we can obtain highly significant computational savings, in terms of the total processing time, through the use of the ray density provided the proposed bound. Our second set of experiments illustrates this.

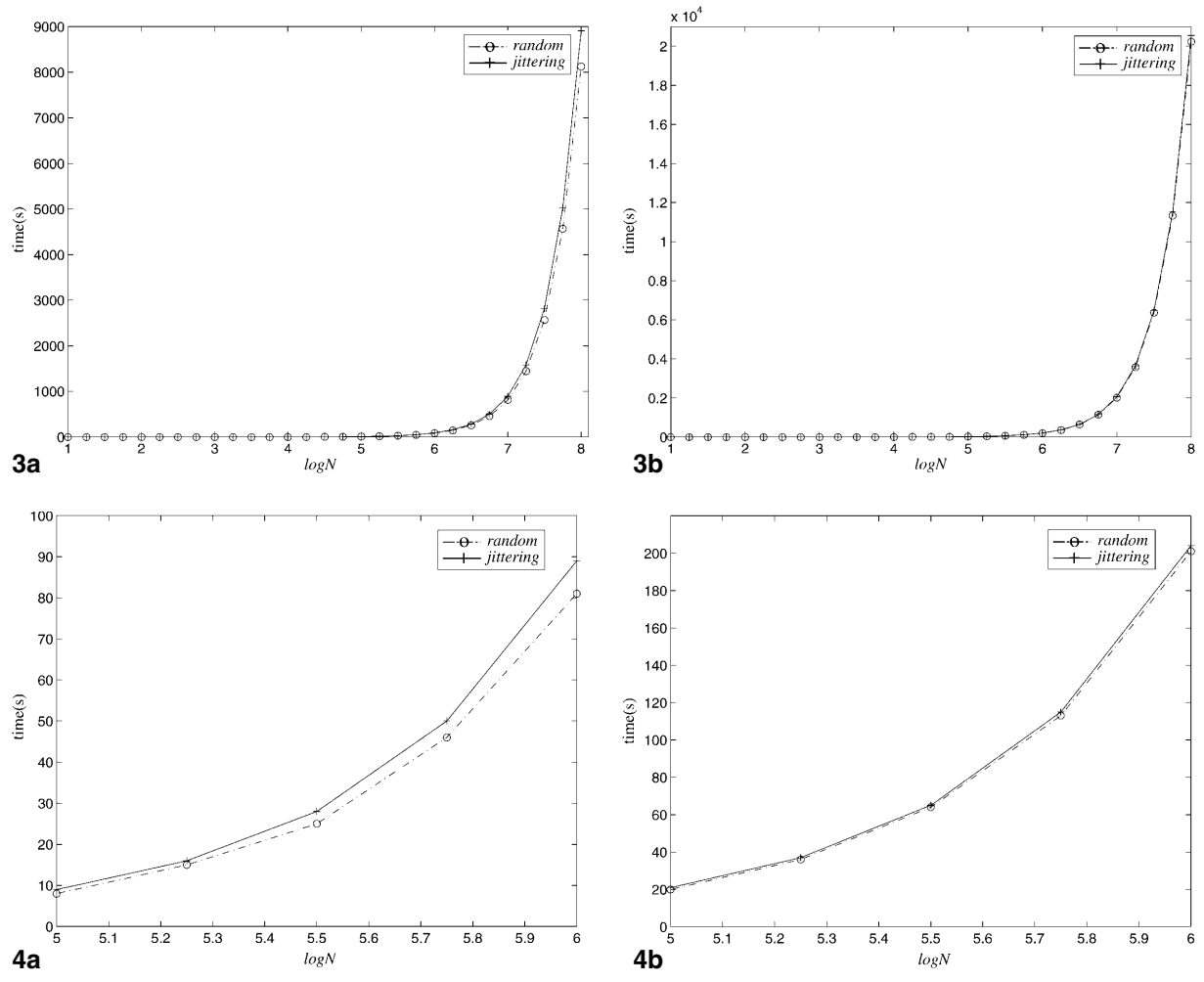

Fig. 3a,b. Processing times (given by elapsed CPU time on an SGI R5000) associated with the virtual spectrophotometric measurements for: **a** the simplified reflectance model for dielectrics; **b** the algorithmic reflectance model for plant leaves
Fig. 4a,b. Close-up of the curve of processing times associated with the measurements for: **a** the simplified reflectance model for dielectrics; **b** the algorithmic reflectance model for plant leaves

5.3 Measurements of directional-hemispherical reflectance

Figures 5 and 6 show the results of directional-hemispherical reflectance measurements when $\phi_i = 0°$ and $\theta_i \in [0°, 90°]$ is sampled at intervals of 1°. For applications involving a large number of measurement instances, such as these, we need to select a ray density that allows minimal fluctuations in the resulting curves. As we can see in Fig. 5, for $N = 10^3$ (or $\log N = 3$) we have very noticeable fluctuations. As we increase the value of N, we start to have smoother curves, and for $N = 10^5$ (or $\log N = 5$) the curves present negligible fluctuations. We can reduce the fluctuations even more by increasing the value of N, e.g., using $N = 10^6$ (or $\log N = 6$). The graph of the average magnitude of fluctuations, computed using (24) and presented in Fig. 6a, shows, however, that in this case we would have only a minor reduction in the fluctuations for both reflectance models. Moreover, the graph presented in Fig. 6b shows that in this case we would

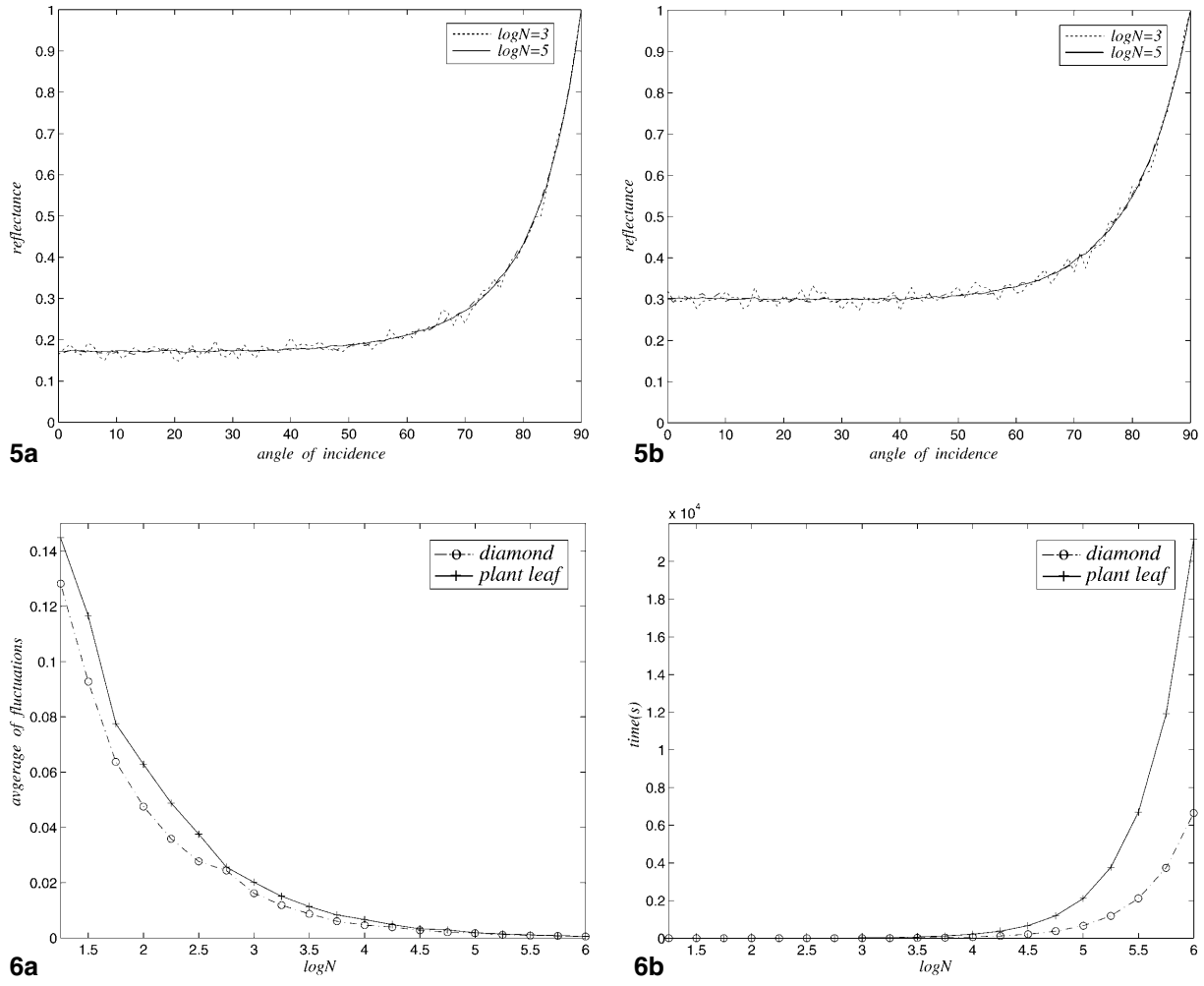

Fig. 5a,b. Directional-hemispherical reflectance measurements using two different ray densities for: **a** the simplified reflectance model for dielectrics ($\eta_{\text{diamond}} = 2.419$); **b** the algorithmic reflectance model for plant leaves ($\lambda = 551$ nm)
Fig. 6. a Average of fluctuations and **b** processing times (given by elapsed CPU time on an SGI R5000) associated with the directional-hemispherical reflectance measurements for the two reflectance models used in our experiments

have a substantial increase in the processing time (around 10 ×) for both reflectance models. These observations suggest that we can obtain results with a reasonably high reliability/cost ratio using the ray density given by the proposed bound (23) for applications of this type as well.

6 Conclusion

The reliability and efficiency of virtual spectrophotometers are directly determined by an appropriate qualitative and quantitative selection of sample rays, which is required to obtain estimates with a desired accuracy under specified spectral and geometrical conditions. The application of a brute-force approach to determine the ray density which may ensure results within the region of constant convergence is highly inefficient. We therefore investigated alternatives to obtain satisfactory bounds for the ray density needed for a virtual spectrophotometer. Such a bound should take into account the accuracy and performance requirements of rendering applications.

As a result of this investigation we proposed a bound derived from the exponential Chebyshev inequality. This bound provides tighter ray densities than previous probability theory results used in particle transport formulations. The application of this inequality also does not require the pre-estimation of variances usually required in the evaluation of accuracy of Monte Carlo methods used in rendering applications.

Experiments were performed using different sampling strategies, random and stratified (jittering), and models of reflectance with different levels of complexity to illustrate the applicability of the proposed bound. These experiments suggest that the proposed bound allows us to obtain results with a reasonably high reliability/cost ratio and show that the suitability of the proposed bound becomes even more noticeable for applications involving a large number of measurement instances. In many cases the total computation time can be reduced by several orders of magnitude through the application of the proposed bound.

The main purpose of this research was to contribute to a better theoretical foundation for fundamental research required for biologically and physically based rendering applications. However, the techniques presented in this work can be applied to other areas demanding virtual spectrophotometric measurements such as remote sensing and colorimetry. Viewed in this context, this work seems to follow the guideline suggested by Greenberg [16, 30]:

> If computer graphics is to have a role in improving the future of our civilization, the real value will be in its application to science, engineering and design.

Our future efforts will be focus on the ray density analysis for virtual devices measuring the spatial distribution of light, known as goniophotometers. We also intend to investigate the application of the exponential Chebyshev inequality to other rendering problems involving particle transport simulation such as the computation of form factors [6].

Acknowledgements. Thanks are due to Mark Tigges for the question that triggered the research for this paper and to the anonymous referees for their valuable comments. Thanks are also due to the National Science and Research Council of Canada for funding the postdoctoral fellowship of the first author and the operating grant of the second author.

References

1. ANSI (1986) Nomenclature and definitions for illuminating engineering, ANSI/IES RP-16-1986. Illuminating Engineering Society of North America, New York
2. ASTM (1992) ASTM Standard E284-91C. Standard terminology of appearance. In: LB Wolff, SA Shafer, GE Healey (eds) Physics-based vision principles and practice: radiometry. Jones and Bartlett, Boston, pp 146–161
3. Baranoski GVG, Rokne JG (1997) An algorithmic reflectance and transmittance model for plant tissue. Comput Graph Forum (EUROGRAPHICS Proceedings) 16(3):141–150
4. Baranoski GVG, Rokne JG (1999) A nondeterministic reconstruction approach for isotropic reflectances and transmittances. J Visualization Comput Anim 10(4):225–231
5. Baranoski GVG, Rokne JG (2001) Efficiently simulating scattering of light by leaves. Visual Comput (in press)
6. Baranoski GVG, Rokne JG, Xu G (2001) Applying the exponential Chebyshev inequality to the nondeterministic computation of form factors. J Quant Spectrosc Radiat Transfer (in press)
7. Baranoski GVG, Rokne JG, Xu G (2000b) Virtual spectrophotometric measurements for biologically and physically-based rendering. In: Proceedings of the Eighth Pacific Conference on Computer Graphics and Applications – Pacific Graphics '2000, Hong Kong, October. IEEE Computer Society, pp 398–399
8. Carter L, Cashwell ED (1975) Particle transport simulation with the Monte Carlo method. Technical report, Energy Research and Development Administration
9. Cashwell ED, Everett CJ (1959) A practical manual on the Monte Carlo method for random walk problems. Pergamon, New York
10. Chiang CL (1980) An introduction to stochastic processes and their applications. Krieger, Huntington, NY
11. Corson-Rikert J (2000) Report of the Workshop on Rendering, Perception and Measurement. Comput Graph 34(1):37–39
12. Crowther BG (1996) Computer modeling of integrating spheres. Appl Opt 35(30):5880–5886
13. Glassner AS (1995) Principles of Digital Image Synthesis. Morgan Kaufmann, San Francisco
14. Goebel DG (1967) Generalized integrating-sphere theory. Appl Opt 6(1):125–128
15. Govaerts YM, Jacquemoud S, Verstraete M, Ustin SL (1996) Three-dimensional radiation transfer modeling in a dycotyledon leaf. Appl Opt 35(33):6585–6598
16. Greenberg DP (1987) The 1987 Steven A. Coons Award Lecture. Comput Graph 22(1):15
17. Hanrahan P, Krueger W (1993) Reflection from layered surfaces due to subsurface scattering. Comput Graph (SIGGRAPH Proceedings), pp 165–174
18. Hecht E, Zajac A (1974) Optics. Addison-Wesley, Reading, MA
19. Hosgood B, Jacquemoud S, Andreoli G, Verdebout J, Pedrini G, Schmuck G (1995) Leaf optical properties experiment 93. Technical Report EUR 16095 EN, Joint Research Centre, European Comission, Institute for Remote Sensing Applications

20. Hunter RS, Harold RW (1987) The measurement of appearance, 2nd edn. Wiley, New York
21. Judd DB, Wyszecki G (1975) Color in business, science and industry, 3rd edn. Wiley, New York
22. Lalonde P, Fournier A (1997) A wavelet representation of reflectance functions. IEEE Trans Visualization Comput Graph 3(4):329–336
23. MacAdam DL (1981) Color measurement: theme and variations. Springer, Berlin Heidelberg New York
24. Nicodemus FE, Richmond JC, Hsia JJ, Ginsberg IW, Limperis T. (1992) Geometrical considerations and nomenclature for reflectance. In: Wolff LB, Shafer SA, Healey GE (eds) Physics-based vision principles and practice: radiometry. Jones and Bartlett, Boston, pp 94–145
25. Nievergelt Y (1997) Radiosity in illuminating engineering. UMAP J 18(2):167–179
26. Shirley P (1990) Physically based lighting for computer graphics. PhD thesis, Dept of Computer Science, University of Illinois
27. Shiryaev AN (1996) Probability, 2nd edn. Springer, New York
28. Uspensky JV (1937) Introduction to mathematical probability. McGraw-Hill, New York
29. Zerlaut GA, Anderson TE (1981) Multiple-integrating sphere spectrophotometer for measuring absolute spectral reflectance and transmittance. Appl Opt 20(21):3797–3804
30. Watt W, Watt M (1992) Advanced animation and rendering techniques theory and practice. ACM Press, New York, p 298

GLADIMIR BARANOSKI is a faculty member at the University of Waterloo. He received his PhD in computer science from the University of Calgary in 1998. The main topic of his doctoral research was the development of reflectance and scattering models for plants. As a postdoctoral fellow at the University of Utah he continued to work on the modeling and rendering of natural phenomena. His research interests include biologically and physically based rendering, simulation of natural phenomena and the development of practical solutions for radiative transfer problems. He is a member of ACM (SIGGRAPH).

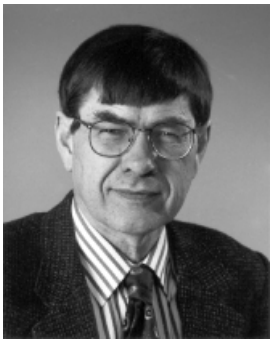

JON ROKNE was born in Bergen, Norway, in 1941. He is currently a professor and former head of the Computer Science Department at the University of Calgary, Canada, where he has been a faculty member since 1970. He has been a visiting professor at the Universities of Canterbury, New Zealand (1978), Freiburg, Germany (1980), Grenoble, France (1983–84) and Karlsruhe, Germany (1984). He holds a PhD in mathematics from the University of Calgary (1969). His research interests span interval analysis, computer graphics and global optimization.

GUANGWU XU has a PhD in mathematics. He has been working in various fields including cryptography, harmonic analysis, categorical computation, formal language theory and computer graphics.